

## Compact amorphous-silicon visible-light monitor integrated in silicon nitride waveguides

De Vita, Christian; Klitis, Charalambos; Codreanu, Nina; Ferrari, Giorgio; Sorel, Marc; Melloni, Andrea; Morichetti, Francesco

**DOI**

[10.1109/GFP51802.2021.9673949](https://doi.org/10.1109/GFP51802.2021.9673949)

**Publication date**

2022

**Document Version**

Final published version

**Published in**

2021 IEEE 17th International Conference on Group IV Photonics, GFP 2021 - Proceedings

**Citation (APA)**

De Vita, C., Klitis, C., Codreanu, N., Ferrari, G., Sorel, M., Melloni, A., & Morichetti, F. (2022). Compact amorphous-silicon visible-light monitor integrated in silicon nitride waveguides. In *2021 IEEE 17th International Conference on Group IV Photonics, GFP 2021 - Proceedings* (IEEE International Conference on Group IV Photonics GFP; Vol. 2021-December). IEEE. <https://doi.org/10.1109/GFP51802.2021.9673949>

**Important note**

To cite this publication, please use the final published version (if applicable). Please check the document version above.

**Copyright**

Other than for strictly personal use, it is not permitted to download, forward or distribute the text or part of it, without the consent of the author(s) and/or copyright holder(s), unless the work is under an open content license such as Creative Commons.

**Takedown policy**

Please contact us and provide details if you believe this document breaches copyrights. We will remove access to the work immediately and investigate your claim.

***Green Open Access added to TU Delft Institutional Repository***

***'You share, we take care!' - Taverne project***

**<https://www.openaccess.nl/en/you-share-we-take-care>**

Otherwise as indicated in the copyright section: the publisher is the copyright holder of this work and the author uses the Dutch legislation to make this work public.

# Compact amorphous-silicon visible-light monitor integrated in silicon nitride waveguides

Christian De Vita<sup>1</sup>, Charalambos Klitis<sup>2</sup>, Nina Codreanu<sup>1,3</sup>, Giorgio Ferrari<sup>1</sup>, Marc Sorel<sup>2</sup>, Andrea Melloni<sup>1</sup>, Francesco Morichetti<sup>1</sup>

<sup>1</sup>Department of electronics, information and bioengineering (DEIB), Politecnico di Milano, 20133 Italy

<sup>2</sup>University of Glasgow, Rankine Building, Oakfield Avenue, Glasgow G12 8LT, UK

<sup>3</sup>Now with: QuTech/Department of Quantum Nanoscience and Kavli Institute of Nanoscience, Delft University of Technology, Delft, The Netherlands

[christian.devita@polimi.it](mailto:christian.devita@polimi.it)

**Abstract**—This work reports on the realization of an amorphous silicon visible-light detector integrated in Si<sub>3</sub>N<sub>4</sub> waveguides. The device is very compact (< 40 μm), has a responsivity of about 10 mA/W and a sensitivity of -40 dBm.

**Keywords**—optical waveguides, amorphous silicon, integrated detectors, visible light, photonic integrated circuits

## I. INTRODUCTION

Visible-light is a spectral region of much interest for many applications such as imaging, metrology, biosensing, nanomedicine and quantum optics. In this wavelength range, Silicon Nitride (SiN) is one of the most established high-contrast photonic platforms, offering a good tradeoff between low propagation loss and high integration scale [1]. In order to make photonic integrated circuits evolve towards more complex programmable architectures [2], it is necessary to monitor the working point of the photonic device by means of on-chip in-line light detectors.

Amorphous silicon (a-Si) is widely used in the visible range for the realization of opto-electronic devices, such as in photovoltaic applications. In integrated optics, a-Si is employed to realize optical waveguides for the near-infrared range where it is almost transparent, but in the visible range it is still largely unexploited. The integration of an a-Si detector on a lithium niobate waveguide on silicon has been recently demonstrated at 850 nm wavelength [3]. In this work, we exploit the photoconductivity of an a-Si film deposited as a coating layer of a SiN waveguide to realize a compact in-line photodetector operating in the red-light range. A sensitivity down to -40 dBm with a responsivity of 10mA/W is demonstrated.

## II. ASSESSMENT OF A-SI PHOTOCONDUCTIVITY

The a-Si layer was deposited with a Silane based PECVD deposition: the presence of SiH<sub>4</sub> will ensure the hydrogenation of the a-Si film, at the base of the photoconductive properties of amorphous the Silicon films [4]. An optimization process was performed in order to maximize the absorption coefficient of the a-Si film in the entire visible range of wavelengths in order to achieve the highest photoconductive response of the material. Material deposition was carried out with an RF power of 50W at 13.56MHz, a chamber pressure of 500 mTorr and a substrate temperature of 300°C.

The photoconductivity of the a-Si thin film at a wavelength  $\lambda = 660$  nm was assessed by means of the vertically-illuminated

test device shown in Fig 1(a). The Au/Cr electrodes were realized through a lift-off process, by using direct laser writing lithography followed by a thermal evaporation process. As shown in Fig. 1(b), the light beam is vertically shone on the photoconductive film from a single-mode optical fiber, while two metallic probes are used to feed the device electrodes with the bias voltage and to read the light-dependent current through a lock-in read-out scheme. The I-V characteristics was firstly measured in DC in dark condition, this measurement providing a dark conductivity of the a-Si film of about 10<sup>-7</sup> S/cm. Upon illumination see [Fig. 1(c)], we observed a dynamic range in the measured power intensity higher than 40 dB (from -50 dBm to -10 dBm), this change being responsible for a variation of more than three orders of magnitude in the a-Si conductivity (quantified in about 10<sup>-4</sup> S/cm for -9 dBm input power). The slight sublinearity in the current-power characteristic is due to the reduction of the free-carrier lifetime in the a-Si film at high carrier generation rate, that is at higher photon flux) [4].

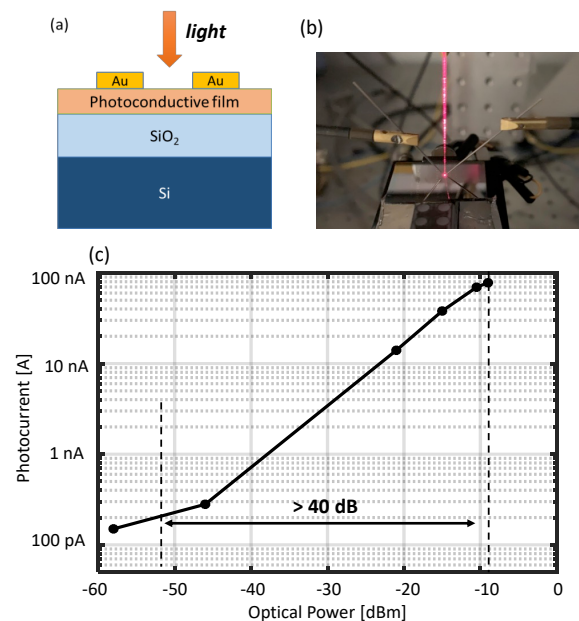


Figure 1. (a) Schematic of the vertically-illuminated device for the assessment of a-Si photoconductivity. (b) Photograph of the experimental setup. (c) Photocurrent measured in vertically-illuminated test devices (electrode size 200 μm x 200 μm, electrode spacing 20 μm) for increasing optical power at a wavelength of 660 nm (red light).

This effect is responsible for a reduction of the responsivity at higher optical power; however, at maximum optical power of -9 dBm, a photocurrent of 80 nA is measured (20  $\mu\text{m}$  electrode spacing, 8V applied voltage) resulting in a responsivity of about 5 mA/W, which is close to recently reported results for a-Si photoconductors [3].

### III. A-SI DETECTOR INTEGRATED IN $\text{Si}_3\text{N}_4$ WAVEGUIDES

Figure 2(a) schematically shows the longitudinal geometry of the a-Si detector integrated in  $\text{Si}_3\text{N}_4$  waveguide. The hydrogen silsesquioxane (HSQ) upper cladding of a buried channel waveguide ( $\text{Si}_3\text{N}_4$  core 400 nm x 200 nm) is locally lowered in order to enable the deposition of a thin film of a-Si at a suitable spacing from the waveguide in order to introduce a controllable absorption of the guided light. Electromagnetic simulations based on the beam propagation method (BPM) show that the evanescent coupling between the fundamental transverse electric (TE) mode and a 200 nm thick a-Si film coating layer at a distance of 200 nm provides 4 dB absorption over 100  $\mu\text{m}$  propagation length. Figure 2(b) shows a top view microphotograph of a fabricated device. Selective removal of the HSQ upper cladding was performed by direct laser writing optical lithography followed by reactive ion etching in  $\text{CHF}_3/\text{O}_2$  mixture. Once deposited, the a-Si is then patterned by direct laser writing optical lithography and then dry etched in  $\text{SF}_6/\text{O}_2$  mixture. On top of the a-Si film a pair of electric contact pads (4  $\mu\text{m}$  spacing, 15  $\mu\text{m}$  width) were fabricated by lift-off technique using a direct laser writing optical lithography followed by the deposition of 150 nm of gold with a small adhesion layer of chromium. The bonded pads are kept as far as possible in order to avoid unwanted capacitances, while the two golden paths are kept very close in order to minimize the resistive path of the current in the a-Si.

The laser source is butt-coupled to the waveguide device by using a horizontal alignment optical setup. The optical fiber has a mode field diameter of about 3.5  $\mu\text{m}$  (+/-0.5) providing a coupling loss of about 10 dB/facet with the optical waveguide if no mode adapters are realized at the waveguide termination. In order to reduce the parasitic capacitances due to the electrical probes, the sample was wire bonded to an electrical. Figure 2(c) shows the measured photocurrent versus the frequency of the lock-in read-out for different optical power in the detector region. The plateau in the low-frequency side of the curves provides the light dependent change of the photocurrent due to the photoconductivity of the a-Si film, whereas the high frequency behavior is dominated by the parasitic capacitance between the metallic pads. The black line provides a reference dark current of 65 pA (at 8 V applied voltage). When the light beam is switched on, a photocurrent of about 4 nA is measured (red line), with an estimated power at the sensor of -30 dBm and an absorption of 2 dB. This photocurrent corresponds to a responsivity of about 10 mA/W, that is similar to the one we obtained for the vertically illuminated device. The maximum frequency of the detector is currently set by the parasitic capacitance limiting the operational bandwidth to 1 kHz at -30 dBm, which is however in line with typical monitoring operation

but that can be used down to almost -50 dBm with longer reading time

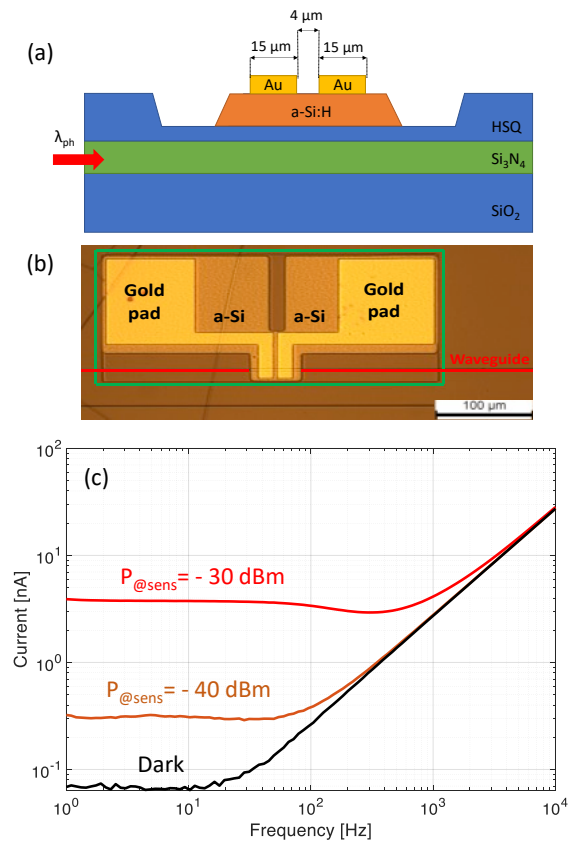


Figure 2. (a) Schematic of the a-Si detector integrated in a  $\text{Si}_3\text{N}_4$  waveguide; (b) Top view photograph of a fabricated device; (c) Measured photocurrent versus the frequency of the electrical lock-in read-out for increasing optical power at the detector: dark condition (black curve), -40 dBm (brown), and -30 dBm (red curve).

### ACKNOWLEDGMENT

We acknowledge Stefania Intelisano and the technical staff of the JWNC at Glasgow University and of Polifab, the micro- and nanofabrication facility of Politecnico di Milano, for support in the fabrication of the devices. This supported by European Commission through H2020 grant number 829116 (Super-Pixels).

### REFERENCES

- [1] Wesley D. Sacher et al. "Visible-light silicon nitride waveguide devices and implantable neurophotonic probes on thinned 200 mm silicon wafers," *Opt. Express* 27, 37400-37418 (2019)
- [2] Bogaerts, W., Pérez, D., Capmany, J. et al. Programmable photonic circuits. *Nature* 586, 207-216 (2020). <https://doi.org/10.1038/s41586-020-2764-0>
- [3] B. Desiatov and M. Loncar. "Silicon photodetector for integrated lithium niobate photonics". *Appl. Phys. Lett.* 115, 121108 (2019).
- [4] C. R. Wronski and R. E. Daniel, "Photoconductivity, trapping, and recombination in discharge-produced, hydrogenated amorphous silicon," *Phys. Rev. B* 23, 794 (1981).